Phases of the (2+1) Dimensional SO(5) Nonlinear Sigma Model with Topological Term

Zhenjiu Wang,[1,*] Michael P. Zaletel,[2] Roger S. K. Mong,[3] and Fakher F. Assaad[1,4,†]
[1]*Institut für Theoretische Physik und Astrophysik, Universität Würzburg, 97074 Würzburg, Germany*
[2]*Department of Physics, University of California, Berkeley, California 94720, USA*
[3]*Department of Physics and Astronomy, University of Pittsburgh, Pittsburgh, Pennsylvania 15260, USA*
[4]*Würzburg-Dresden Cluster of Excellence ct.qmat, Am Hubland, D-97074 Würzburg, Germany*

(Received 26 March 2020; accepted 5 January 2021; published 29 January 2021)

We use the half-filled zeroth Landau level in graphene as a regularization scheme to study the physics of the SO(5) nonlinear sigma model subject to a Wess-Zumino-Witten topological term in $2+1$ dimensions. As shown by Ippoliti *et al.* [Phys. Rev. B **98**, 235108 (2019)], this approach allows for negative sign free auxiliary field quantum Monte Carlo simulations. The model has a single free parameter U_0 that monitors the stiffness. Within the parameter range accessible to negative sign free simulations, we observe an ordered phase in the large U_0 or stiff limit. Remarkably, upon reducing U_0 the magnetization drops substantially, and the correlation length exceeds our biggest system sizes, accommodating 100 flux quanta. The implications of our results for deconfined quantum phase transitions between valence bond solids and antiferromagnets are discussed.

DOI: 10.1103/PhysRevLett.126.045701

Introduction.—At critical points the renormalization group allows for the definition of emergent symmetries and field theories. For example, the semimetal to insulator transitions in graphene [1–3] have an emergent Lorentz symmetry [4,5] so that space and time can interchangeably be used [6] to efficiently compute critical exponents. Models that capture the physics of deconfined quantum criticality (DQC) [7,8]—the JQ model, for example [9]—have an $\mathrm{SO}(3)\times C_4$ symmetry, but at criticality the C_4 point group is enlarged to a higher U(1) symmetry. Improved models, with $\mathrm{SO}(3)\times \mathrm{U}(1)$ symmetry have been proposed to study DQC [10]. Formulating the theory of DQC with eight component Dirac fermions akin to graphene and Yukawa coupled to a quintuplet of anti-commuting mass terms [11] quite naturally leads to the conjecture of an emergent SO(5) symmetry [12–14]. Compelling numerical evidence for this emergent symmetry has been put forward [15] in the realm of loop models [16].

Let us now consider a phase transition with enhanced symmetry and a relevant operator α that breaks it. In this case, formulating a model with higher symmetry allows us to assess the nature of the transition. Schematic RG flows for an enhanced SO(5) symmetry that is broken down to $\mathrm{SO}(3)\times\mathrm{SO}(2)$ are shown in Fig. 1. While α breaks the SO(5) symmetry, U_0 conserves it. If the higher symmetry model is in an ordered phase, then the transition is first order [Fig. 1(a)]. The spin-flop transition corresponding to the field-driven reorientation of the easy axis falls into this category. Alternatively, the enhanced symmetry model can be critical such that the transition is continuous [Fig. 1(b)]. As an example for this scenario, we can consider the one-dimensional DQC between a dimer and Néel state in the XXZ model considered in Refs. [17,18] and realized in Ref. [19]. The critical point has a U(1) symmetry that is broken by the umklapp operator that tunes through the transition. As a third possibility, the enhanced-symmetry

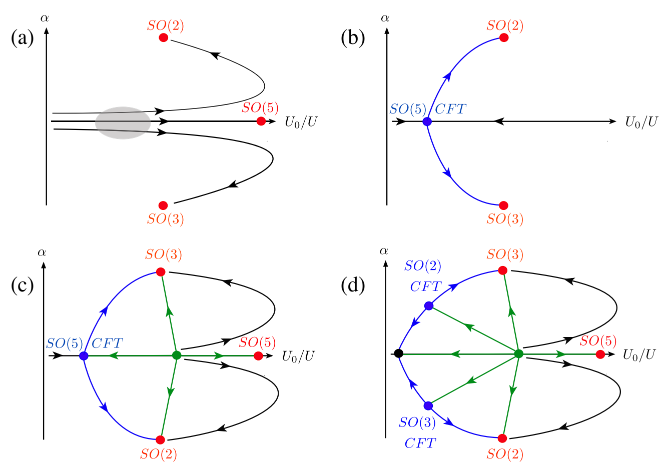

FIG. 1. Possible RG flows in the U_0 versus α phase. α corresponds to the amplitude of a term that breaks down the SO(5) symmetry to $\mathrm{SO}(3)\times\mathrm{SO}(2)$. The horizontal line corresponds to the $\alpha=0$ or to SO(5) symmetry. Red bullets, corresponds to phases where the symmetry group is spontaneously broken. The black bullet is an SO(5) disordered phase. Blue (green) bullets denote critical (multi-critical) points. In scenario (a) the SO(5) model orders and the shaded region depicts a slow RG flow (see text). In (b) the SO(5) model remains critical. In (c) the SO(5) model has an ordered and critical phase separated by a multi-critical point. Finally, in (d) the SO(5) model shows an order-disorder transition.

model may have a relevant tuning parameter U_0—and associated (multi) critical point—that does not break the enhanced symmetry. Figure 1(c) describes a scenario where the ordered state gives way to a critical phase. In this case, tuning α leads to first order or continuous transitions depending upon the value of U_0. Finally, in Fig. 1(d) U_0 drives an order-disorder transition. Aside from fine-tuning, the transition from the SO(3) to SO(2) broken symmetry states is first order or separated by a disordered phase.

The aim of this Letter is to investigate the O(5) nonlinear sigma model in $2+1$ dimensions with a Wess-Zumino-Witten geometrical term. As mentioned above, this model can be obtained by integrating out quintuplets of anti-commuting mass terms in Dirac systems [12–14],

$$S = \frac{1}{g}\int d^3x(\nabla\hat{\boldsymbol{\varphi}})^2 + S_{\mathrm{WZW}} + \cdots \tag{1}$$

where ellipsis refer to higher order nongeometrical terms. Here $\hat{\boldsymbol{\varphi}}$ corresponds to a five-dimensional unit vector. The model has a manifest SO(5) symmetry, and a single parameter, the stiffness. The question we would like to address in this work is the nature of the phase diagram as a function of the stiffness.

Model and method.—The work of Ippoliti *et al.* [20] demonstrates that a nonlinear sigma model with exact SO (5) symmetry can be constructed using 8 component Dirac fermions quenched in the zeroth Dirac Landau level (ZLL). As opposed to a lattice approach, one remains in continuum space time, but the single particle Hilbert space remains finite and counts the $4N_\phi$ states of the ZLL, where N_ϕ is the number of magnetic fluxes piercing the two dimensional space. The model reads

$$\hat{H} = \int_V d^2\boldsymbol{x}\left(\frac{U_0}{2}[\hat{\boldsymbol{\psi}}^\dagger(\boldsymbol{x})\hat{\boldsymbol{\psi}}(\boldsymbol{x}) - C(\boldsymbol{x})]^2 - \frac{U}{2}\sum_{i=1}^{5}[\hat{\boldsymbol{\psi}}^\dagger(\boldsymbol{x})O^i\hat{\boldsymbol{\psi}}(\boldsymbol{x})]^2\right), \tag{2}$$

where the fermion annihilation operator are projected onto the ZLL: $\hat{\psi}_a(\boldsymbol{x}) = \sum_{k=1}^{N_\phi}\phi_k(\boldsymbol{x})\hat{c}_{a,k}$. The index a runs from $1\cdots 4$ corresponding to the four Dirac ZLLs. It is crucial that the operators $\hat{\boldsymbol{\psi}}(\boldsymbol{x})$ $[\hat{\boldsymbol{\psi}}^\dagger(\boldsymbol{x})]$ do not satisfy the canonical commutation rules due to the projection. The wave functions of the ZLL, $\phi_{k_y}(\boldsymbol{x})$, are computed in the Landau gauge which diagonalizes the translation invariance along one direction (see Supplemental Material [21]). The background $C(\boldsymbol{x}) \equiv 2\sum_{k_y=1}^{N_\phi}|\phi_{k_y}(\boldsymbol{x})|^2$ ensures particle-hole symmetry in Eq. (2).

For $i = 1\ldots 5$, O^i, are mutually anticommuting matrices. A convenient choice reads

$$\tau_x \otimes \mathbb{I}_2, \tau_y \otimes \mathbb{I}_2, \tau_z \otimes \vec{\tau} \quad i = 1, 2, \ldots 5. \tag{3}$$

The 10 matrices $L^{ij} = -(i/2)[O^i, O^j]$, $i, j = 1\ldots 5$, are the generators of the SO(5) group and commute with the Hamiltonian. Along the SO(5) high symmetry line, the Hamiltonian has only one energy scale U_0/U.

Let $\varphi_i(\boldsymbol{x}) = \langle\hat{\boldsymbol{\psi}}^\dagger(\boldsymbol{x})O^i\hat{\boldsymbol{\psi}}(\boldsymbol{x})\rangle$ and assume that the mass gap $\Delta \propto |\boldsymbol{\varphi}|$ is finite. One can then omit amplitude fluctuations of the vector $\boldsymbol{\varphi}(\boldsymbol{x})$, integrate out the fermions in the large mass approximation to obtain an effective field theory for $\hat{\boldsymbol{\varphi}}(\boldsymbol{x}) \equiv \boldsymbol{\varphi}(\boldsymbol{x})/|\boldsymbol{\varphi}(\boldsymbol{x})|$ that corresponds precisely to Eq. (1) [21,22]. We measure lengths in units of the magnetic length l_B and energies in units of U. Our model has only one dimensionless parameter U_0/U, such $1/g$ can only depend on this quantity. An explicit form, originating from a gradient expansion, showing that $1/g$ is a monotonically increasing function of U_0/U, is given in the Supplemental Material [21].

As mentioned previously, our numerical simulations are based on the work of Ippoliti *et al.* [20] that shows how to formulate a negative sign free auxiliary field QMC for the Hamiltonian of Eq. (2) in the parameter range $U_0/U \geq -1$. The algorithm is formulated in Fourier space,

$$\hat{H} = \frac{1}{2V}\sum_{\boldsymbol{q}}\left(U_0\hat{n}(\boldsymbol{q})\hat{n}(-\boldsymbol{q}) - U\sum_{i=1}^{5}\hat{n}^i(\boldsymbol{q})\hat{n}^i(-\boldsymbol{q})\right), \tag{4}$$

with $\hat{\boldsymbol{\psi}}^\dagger(\boldsymbol{x})O^i\hat{\boldsymbol{\psi}}(\boldsymbol{x}) = (1/V)\sum_{\boldsymbol{q}} e^{-i\boldsymbol{q}\cdot\boldsymbol{x}}\hat{n}^i(\boldsymbol{q})$ and $\hat{\boldsymbol{\psi}}^\dagger(\boldsymbol{x})\hat{\boldsymbol{\psi}}(\boldsymbol{x}) - C(\boldsymbol{x}) = (1/V)\sum_{\boldsymbol{q}} e^{-i\boldsymbol{q}\cdot\boldsymbol{x}}\hat{n}(\boldsymbol{q})$. As shown in the Supplemental Material [21] one key point is to use a Fierz identity to avoid the negative sign problem. For each $\boldsymbol{q}$ we then use a complex Hubbard-Stratonovich transformation to decouple the interaction term. Auxiliary field QMC simulations turn out to be involved. The difficulty lies in the fact that the projected density operators are not local and that they do not commute with each other. In the Supplemental Material [21] we show that for a symmetric Trotter decomposition, that preserves the hermiticity of the imaginary time propagation, the systematic error scales as $(\Delta\tau N_\phi)^2$. Here we have set the magnetic unit length l_B to unity such that N_ϕ corresponds to the volume. We also note that the SO(5) symmetry is broken by the Trotter decomposition such that it potentially introduces a relevant operator. For all these reasons, great care has to be taken to control the systematic error, and we are obliged to scale $\Delta\tau$ as $1/N_\phi$. A detailed account of the Trotter error is given in the Supplemental Material [21]. Since we are working in the continuum, the sum over momenta is not bounded. However, the density operator contains a factor $e^{-\frac{1}{4}\boldsymbol{q}^2 l_B^2}$ and momenta that exceed a critical value can be safely omitted. Adopting this regularization strategy restricts the sum over momenta to order N_ϕ values again for the case $l_B = 1$. Again, a detailed test of the choice of the momenta cutoff is given in the Supplemental Material [21]. Taking all the above into account yields a computational effort that scales as $N_\phi^5\beta$ where β is the inverse temperature. This should be

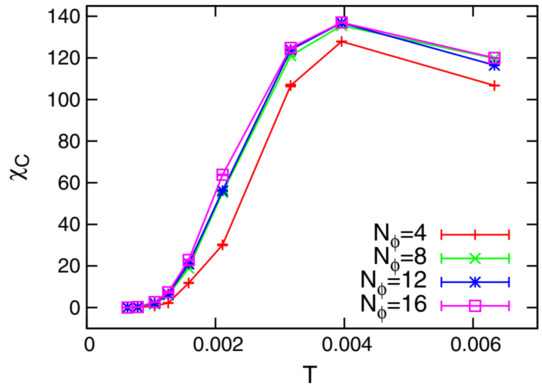

FIG. 2. Temperature dependence of the uniform charge susceptibility χ_C for $U_0 = -1$.

compared to the generic $N_\phi^3 \beta$ scaling for say the Hubbard model. The above explains why our simulations are limited to $N_\phi = 100$. We have used the finite temperature auxiliary field algorithm [23–25] of the algorithms for lattice fermions (ALF) library [26]. The details of our implementation are discussed in the Supplemental Material [21].

Numerical results.—For the simulations we set the energy scale by choosing $U = 1$, the length scale by choosing $l_B = 1$, and vary U_0 and the volume N_ϕ. We found that an inverse temperature of $\beta = 160\pi^2$ suffices to obtain ground state properties on our largest system sizes, $N_\phi = 100$.

In Fig. 2 we plot the uniform charge susceptibility,

$$\chi_C = \frac{\beta}{N_\phi} (\langle \hat{n}_{\boldsymbol{q}=0} \hat{n}_{\boldsymbol{q}=0} \rangle - \langle \hat{n}_{\boldsymbol{q}=0} \rangle \langle \hat{n}_{\boldsymbol{q}=0} \rangle). \tag{5}$$

The charge fluctuations decay exponentially upon reducing the temperature as expected for an insulating state of matter. Since $\hat{\boldsymbol{\psi}}^\dagger(\boldsymbol{x}) O^i \hat{\boldsymbol{\psi}}(\boldsymbol{x})$ are mass terms, any nonvanishing expectation value of these fermion bilinears φ_i will lead to a charge gap. Owing to the SO(5) symmetry the single particle gap is proportional to the norm of this five component vector $|\boldsymbol{\varphi}|$.

Although $|\boldsymbol{\varphi}|$ is finite, phase fluctuations can destroy ordering. To numerically investigate this possibility, we compute the order parameter correlation function

$$S(\boldsymbol{q}) = \frac{1}{N_\phi} \sum_{i=1}^{5} \langle \hat{n}^i_{\boldsymbol{q}} \hat{n}^i_{-\boldsymbol{q}} \rangle. \tag{6}$$

For an ordering wave vector $\boldsymbol{Q}$, the local moment reads

$$m = \sqrt{\frac{1}{N_\phi} S(\boldsymbol{Q})} \tag{7}$$

and it is convenient to define a renormalization group invariant quantity

$$R \equiv 1 - \frac{S(\boldsymbol{Q} + \Delta \boldsymbol{q})}{S(\boldsymbol{Q})} \tag{8}$$

with $|\Delta \boldsymbol{q}| = (2\pi/\sqrt{N_\phi})$. In the ordered (disordered) phase R converges to unity (zero) and the local moment takes a finite (vanishing) value. At a critical point, the correlation ratio converges to a universal value.

In Fig. 3(a) we plot the correlation ratio R as a function of system size for various values of U_0. For system sizes up to $N_\phi = 20$ all curves scale downwards and would suggest a critical or disordered phase. Beyond $N_\phi = 20$ and for large values of U_0 the correlation ratio changes behavior and grows. The length scale at which this crossover occurs can naturally be interpreted as a measure of the correlation length. For these large values of U_0, a finite size extrapolation of the square of the local moment [see Fig. 3(b)] is consistent with a finite value [see inset of Fig. 3(b)]. In Fig. 3(c) we replot the correlation ratio as a function of U_0. The data is consistent with a crossing at $U_0 \simeq 3$. Below this value, R does not scale to zero, as already seen in Fig. 3(a), and hence signals a phase where the correlation length exceeds our system sizes.

Discussion.—In Fig. 1 we show possible RG flows in the U_0 versus α plane where α corresponds to the amplitude of a term that breaks down the SO(5) symmetry to SO(3) × SO(2).

Figure 1(a) corresponds a scenario where the topological term is irrelevant and the model orders for all values of the stiffness. Taken at face value, our results do not support this point of view. However, we cannot exclude the possibility that an ordered phase with small magnetic moment will occur on larger system sizes. In this case, the transition as a function of α from the SO(3) to SO(2) broken symmetries corresponds to a spin-flop transition.

In contrast in Fig. 1(b) we assume that the SO(5) model corresponds to a CFT. In this case, α is a relevant parameter, and the transition from SO(3) to SO(2) broken symmetry phases is continuous with an emergent SO(5) CFT at the critical point. This SO(5) CFT could be a candidate theory for DQCP. Again in light of our data, this scenario seems unlikely since at large values of U_0 our data supports an ordered phase.

In Fig. 1(c) we assume that the observed ordered phase gives way to a critical phase corresponding to an SO(5) CFT. Note that this two fixed point scenario has been suggested by a ϵ expansion of an effective theory at the boundary of an 3 + 1 D SPT state [27]. Adding the α axis implies that along the SO(5) line we have a multicritical point as well as a critical one. Our data actually favors this scenario: below $U_0 = U_0^c \simeq 3$ the correlation ratio does not seem to scale to zero, and is hence consistent with a critical phase. If such is the case, the nature of the transition

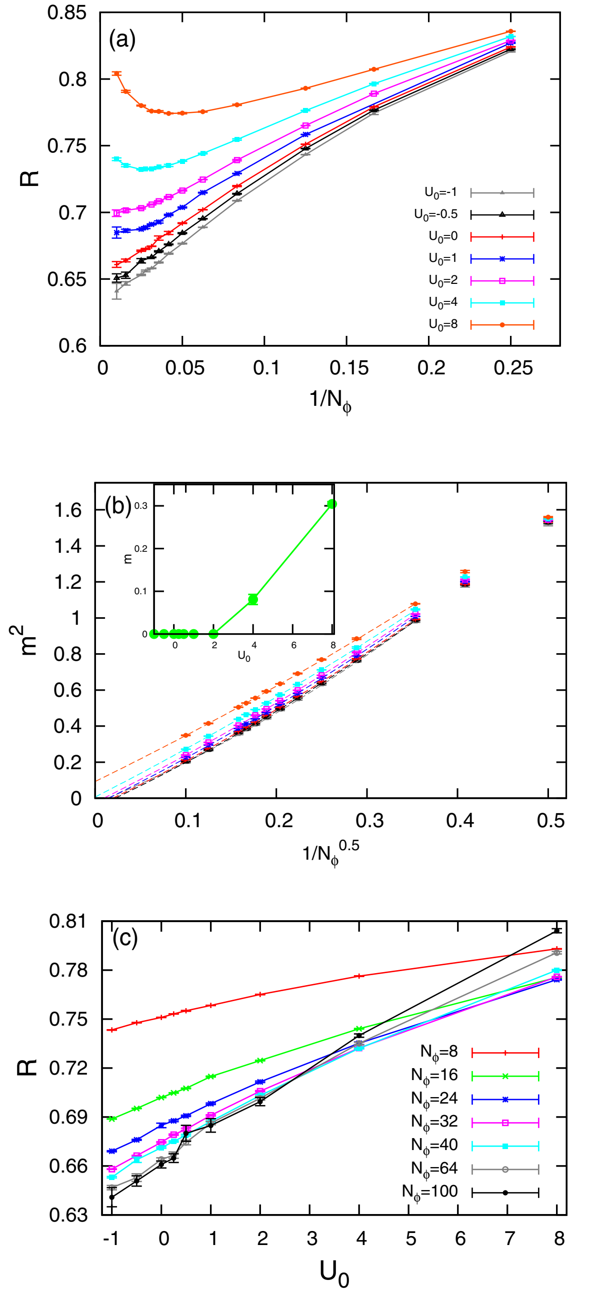

FIG. 3. Correlation ratio R as a function of $1/N_\phi$ (a) and U_0 (c), as well as the O(5) order parameter (b) as a function of $1/\sqrt{N_\phi}$. The dashed lines and the inset is the extrapolation via the fitting form $m(N_\phi)^2 = m^2_{N_\phi\to\infty} + a/\sqrt{N_\phi} + b/N_\phi$. Negative extrapolated values of m^2 suggest a critical or disordered state. In both cases the polynomial, in inverse linear length, fitting form is not justified.

between SO(3) and SO(2) broken symmetry states, with emergent SO(5) symmetry, depends upon the value of U_0 and is either continuous or first order. There are a number of models that show a transition from SO(2) (VBS/SSC) to SO(3) (AFM/QSH) broken symmetry phases and that favor continuous or weakly first order quantum phase transitions. For instance, 3D loop models [16] [$\eta_{\mathrm{Neel}} = 0.259(6)$, $\eta_{\mathrm{VBS}} = 0.25(3)$], the J-Q model, [9,28] as well as transitions between quantum spin Hall insulators and *s*-wave superconductors, [$\eta_{\mathrm{QSH}} = 0.21(5)$, $\eta_{\mathrm{SSC}} = 0.22(6)$] [10] all seem to show similar exponents and are believed to belong to the class of DQCP with emergent spinons coupled to a noncompact U(1) gauge field. Compelling evidence of emergent SO(5) symmetry has been put forward for the loop model [15]. However, the value of the anomalous dimension lies at odds with conformal bootstrap bounds, $\eta > 0.52$ [29], for emergent SO(5) symmetry. Systematic drift in the exponents has been observed in Ref. [16]. Within the present context one can understand the above in terms of fix-point collision put forward in Refs. [30–34]. Consider a third axis—the dimension—and assume that the sketch of Fig. 1(c) is realized *close* to the physical dimension $d = 2$ but that before approaching $d = 2$ the multicritical and critical points collide and develop a complex component. In this case we are back to the spin-flop transition of Fig. 1(a) but with the important insight that the RG flow becomes arbitrarily slow due to proximity of a fix-point collision. The shaded region in Fig. 1(a) schematically depicts the region where the RG flow becomes very slow.

Proximity to a critical point motivates fitting the QMC data to the form $m = m_0 + aN_\phi^{-(\eta+z/4)}$ (see the Supplemental Material [21]). In the region where our correlation length exceeds the size of our system we obtain a good fit with robust anomalous dimension $\eta = 0.28(2)$ under the assumption of $z = 1$ (see the Supplemental Material [21]). The agreement with the aforementioned QMC results is remarkable. We note that this exponent is much larger than the one of the 3D classical O(5) critical point, with $\eta = 0.036(6)$ [35]. We conclude this section by noting that Ref. [36] introduces a fermion model showing a DQCP with emergent SO(5) symmetry and that has exponents that comply with the bootstrap bounds. This model could be a realization of the SO(5) CFT conjectured in Fig. 1(c).

Figure 1(d) describes the possibility of an order-disorder transition along the SO(5) line. Note, however, that on the accessible system sizes, we cannot resolve the length scale associated with the disordered state. This scenario excludes a DQCP with emergent SO(5) symmetry, and the transition from the disordered to ordered phases involve SO(3) or SO (2) critical points. As shown in Fig. 2 the insulating phase has vanishing charge susceptibility. The existence and nature of an SO(5) symmetric disordered phase is intriguing. Starting from Dirac fermions any band insulating state necessarily involves SO(5) symmetry breaking. Hence in the conjectured phase diagram of Fig. 1(d) the disordered phase is not adiabatically connected to a band insulator. In fact, if the disordered phase preserves the particle-hole symmetry, the arguments of Ref. [30] rule out *any* gapped phase (even a topological one), because the particle-hole symmetry forbids the SO(5) Hall-conductance argued to be necessary in any such insulator.

Conclusions.—Our data on systems up to $N_\Phi = 100$ show that the SO(5) nonlinear sigma model exhibits an ordered phase in the limit of large stiffness. Remarkably (and within the accessible parameter range where negative sign free AFQMC simulations can be carried out), we observe another regime characterized by a correlation length that exceeds our system size. Given the aforementioned body of work on DQC and insights from the conformal bootstrap approach, our results find a natural interpretation by assuming that the model lies close to a fix-point with small complex component [30–32] such that the RG flow becomes very slow and shows pseudocritical behavior. Clearly larger system sizes are desirable so as to confirm this point of view. Although very appealing, as implemented the Landau level projection approach comes with a computational effort that scales as $N_\phi^5\beta$ as opposed to $N_\phi^3\beta$ for the generic Hubbard model. Further improvements to the code will have to be implemented so as to reach bigger flux values. The method can also be applied to the O(4) model with θ term at $\theta = \pi$ by setting one mass term to zero. This will have impact on our understanding of easy plane de-confined quantum critical points with emergent O(4) symmetry.

We would like to thank T. Grover, W. Guo, A. Nahum, S. Sachdev, T. Senthil, and C. Wang for discussions, as well as Matteo Ippoliti with whom we have carried out previous work on this subject. The authors gratefully acknowledge the Gauss Centre for Supercomputing e.V. for funding this project by providing computing time on the GCS Supercomputer SUPERMUC-NG at Leibniz Supercomputing Centre. F. F. A. thanks funding from the Deutsche Forschungsgemeinschaft under the Grant No. AS 120/15-1 as well as through the Würzburg-Dresden Cluster of Excellence on Complexity and Topology in Quantum Matter—ct.qmat (EXC 2147, project-id 39085490). Z. W. thanks financial support from the DFG funded SFB 1170 on Topological and Correlated Electronics at Surfaces and Interfaces. M. Z. was supported by the DOE, office of Basic Energy Sciences under Contract No. DEAC02-05-CH11231. R. M. was supported by the National Science Foundation under Grant No. NSF-1848336.

[*]Zhenjiu.Wang@physik.uni-wuerzburg.de
[†]assaad@physik.uni-wuerzburg.de

[1] F. F. Assaad and I. F. Herbut, Phys. Rev. X **3**, 031010 (2013).
[2] F. Parisen Toldin, M. Hohenadler, F. F. Assaad, and I. F. Herbut, Phys. Rev. B **91**, 165108 (2015).
[3] Y. Otsuka, S. Yunoki, and S. Sorella, Phys. Rev. X **6**, 011029 (2016).
[4] D. J. Gross and A. Neveu, Phys. Rev. D **10**, 3235 (1974).
[5] I. F. Herbut, Phys. Rev. Lett. **97**, 146401 (2006).
[6] S. Chandrasekharan and A. Li, Phys. Rev. D **88**, 021701(R) (2013).
[7] T. Senthil, A. Vishwanath, L. Balents, S. Sachdev, and M. P. A. Fisher, Science **303**, 1490 (2004).
[8] T. Senthil, L. Balents, S. Sachdev, A. Vishwanath, and M. P. A. Fisher, Phys. Rev. B **70**, 144407 (2004).
[9] A. W. Sandvik, Phys. Rev. Lett. **98**, 227202 (2007).
[10] Y. Liu, Z. Wang, T. Sato, M. Hohenadler, C. Wang, W. Guo, and F. F. Assaad, Nat. Commun. **10**, 2658 (2019).
[11] S. Ryu, C. Mudry, C.-Y. Hou, and C. Chamon, Phys. Rev. B **80**, 205319 (2009).
[12] A. Abanov and P. Wiegmann, Nucl. Phys. **B570**, 685 (2000).
[13] A. Tanaka and X. Hu, Phys. Rev. Lett. **95**, 036402 (2005).
[14] T. Senthil and M. P. A. Fisher, Phys. Rev. B **74**, 064405 (2006).
[15] A. Nahum, P. Serna, J. T. Chalker, M. Ortuño, and A. M. Somoza, Phys. Rev. Lett. **115**, 267203 (2015).
[16] A. Nahum, J. T. Chalker, P. Serna, M. Ortuño, and A. M. Somoza, Phys. Rev. X **5**, 041048 (2015).
[17] F. D. M. Haldane, Phys. Rev. B **25**, 4925 (1982).
[18] C. Mudry, A. Furusaki, T. Morimoto, and T. Hikihara, Phys. Rev. B **99**, 205153 (2019).
[19] M. Weber, F. Parisen Toldin, and M. Hohenadler, Phys. Rev. Research **2**, 023013 (2020).
[20] M. Ippoliti, R. S. K. Mong, F. F. Assaad, and M. P. Zaletel, Phys. Rev. B **98**, 235108 (2018).
[21] See Supplemental Material at http://link.aps.org/supplemental/10.1103/PhysRevLett.126.045701 for details.
[22] J. Lee and S. Sachdev, Phys. Rev. Lett. **114**, 226801 (2015).
[23] R. Blankenbecler, D. J. Scalapino, and R. L. Sugar, Phys. Rev. D **24**, 2278 (1981).
[24] S. R White, D. J. Scalapino, R. L. Sugar, E. Y. Loh, J. E. Gubernatis, and R. T. Scalettar, Phys. Rev. B **40**, 506 (1989).
[25] F. Assaad and H. Evertz, in *Computational Many-Particle Physics*, edited by H. Fehske, R. Schneider, and A. Weiße, Lecture Notes in Physics Vol. 739 (Springer, Berlin Heidelberg, 2008), pp. 277–356.
[26] M. Bercx, F. Goth, J. S. Hofmann, and F. F. Assaad, SciPost Phys. **3**, 013 (2017).
[27] Z. Bi, A. Rasmussen, Y. BenTov, and C. Xu, arXiv:1605.05336.
[28] H. Shao, W. Guo, and A. W. Sandvik, Science **352**, 213 (2016).
[29] D. Poland, S. Rychkov, and A. Vichi, Rev. Mod. Phys. **91**, 015002 (2019).
[30] C. Wang, A. Nahum, M. A. Metlitski, C. Xu, and T. Senthil, Phys. Rev. X **7**, 031051 (2017).
[31] A. Nahum, Phys. Rev. B **102**, 201116(R) (2020).
[32] R. Ma and C. Wang, Phys. Rev. B **102**, 020407 (2020).
[33] I. F. Herbut and L. Janssen, Phys. Rev. Lett. **113**, 106401 (2014).
[34] Y.-C. He, J. Rong, and N. Su, arXiv:2005.04250.
[35] Q. Liu, Y. Deng, T. M. Garoni, and H. W. Blöte, Nucl. Phys. **B859**, 107 (2012).
[36] Z.-X. Li, S.-K. Jian, and H. Yao, arXiv:1904.10975.